Pure Appl. Chem., Vol. 81, No. 12, pp. 2235–2251, 2009.
doi:10.1351/PAC-CON-09-07-09

Gas adsorption applications of porous metal–organic frameworks*

Shengqian Ma‡

Chemical Sciences and Engineering Division, Argonne National Laboratory, 9700 S. Cass Avenue, Argonne, IL 60439, USA

Abstract: Porous metal–organic frameworks (MOFs) represent a new type of functional materials and have recently become a hot research field due to their great potential in various applications. In this review, recent progress of gas adsorption applications of porous MOFs, mainly including hydrogen storage, methane storage, and selective gas adsorption will be briefly summarized.

Keywords: gas adsorption; hydrogen storage; methane storage; porous metal-organic framework; selective gas adsorption.

INTRODUCTION

Metal–organic frameworks (MOFs) have emerged as a new type of functional materials and have witnessed explosive development and rapid progress over the past 15 years [1]. MOFs, also known as coordination polymers, are highly crystalline inorganic–organic hybrids constructed by assembling metal ions or small metal-containing clusters [known as secondary building units (SBUs)] with multidentate organic ligands (such as carboxylates, tetrazolates, and sulfonates) via coordination bonds. They can be one-, two-, or three-dimensional infinite networks. Of those, three-dimensional MOFs with permanent porosity, which can also be called porous MOFs, are of the greatest interest because the voids inside the frameworks can accommodate guest molecules for a number of applications. Through the judicious selection of the metal ions or SBUs and organic linkers, not only can a variety of topologies and structures be produced [2], but the pore sizes can be systematically tuned and the pore walls can be functionalized for specific applications in catalysis, sensor, gas storage/separation, etc. [3]. This review will focus on the current status of gas adsorption applications of porous MOFs, including hydrogen storage, methane storage, and selective gas adsorption [4].

HYDROGEN-STORAGE APPLICATION OF POROUS MOFS

The dwindling amount of petroleum oil deposits and increasing threat of global warming have prompted the search for alternative clean energy carriers to supplement the current fuel supplies such as petroleum oils, primarily consumed by automobiles. Among various alternatives, hydrogen stands at the forefront due to its clean combustion and high gravimetric energy density [5].

In 2003, the U.S. government launched the Hydrogen Fuel Initiative for developing clean, hydrogen-powered automobiles to replace those currently powered by petroleum oils. The success of com-

Pure Appl. Chem.* **81, 2157–2251 (2009). A collection of invited, peer-reviewed articles by the winners of the 2009 IUPAC Prize for Young Chemists.
‡Fax: +1 630 252 9917; Tel.: +1 630 252 5917; E-mail: sma@anl.gov

mercialization of hydrogen-powered vehicles, however, largely relies on the development of a safe, efficient, and economic on-board hydrogen-storage system. Based on the concept that today's vehicles will be powered by future higher-efficiency hydrogen fuel-cell power sources, the U.S. Department of Energy (DOE) has set a number of targets for the hydrogen-storage system (including the container and necessary ancillary components) [6], and recently revised them as: 0.045 kg/kg or 0.028 kg/l by the year 2010, and 0.055 kg/kg or 0.040 kg/l by the year 2015, and 0.075 kg/kg or 0.070 kg/l as the ultimate values. The kinetics of hydrogen release and recharging must also meet the requirements for practical applications. In other words, the hydrogen adsorption and desorption should be totally reversible, and the recharging of hydrogen should be completed within minutes. In addition, the lifetime of the storage system is targeted at 1000 cycles, to be achieved by 2010, and it needs to be improved to 1500 cycles as the ultimate number by 2015; the storage (or delivery) temperature should range from –40 to 85 °C, and the storage (or delivery) pressure should be less than 100 bar [7]. It is worth noting that the units for the revised DOE gravimetric targets are in units of mass/mass instead of previous wt % [6], because the unit of wt %, which should be equal to (mass H_2)/(mass sample + mass H_2), has unfortunately been frequently misused by neglecting the second term in the denominator, leading to complications in comparing hydrogen uptake capacities of different materials [10]. Therefore, it is recommended that the DOE-revised targets' units of kg/kg and kg/l be used for gravimetric capacity and volumetric capacity, respectively, when reporting hydrogen uptakes in porous MOFs and other porous materials.

Porous MOFs have recently been intensively explored as one of the most promising candidates to approach the DOE targets for on-board hydrogen storage, because of their superior merits such as exceptionally high surface areas, tunable pore sizes, functionalizable pore walls, and well-defined framework–hydrogen interacting sites [8].

In 2003, Yaghi et al. reported the first measurements of hydrogen adsorption on a porous MOF, albeit the exceedingly high uptake of 0.045 kg/kg at 77 K and 1 bar was later revised to 0.0132 kg/kg [9]. Since then, over 200 porous MOFs have been investigated for hydrogen adsorption [10].

Low-pressure cryo-temperature hydrogen-adsorption studies

Although the DOE targets for hydrogen storage are set at the condition of near-ambient temperatures and high pressures, the uptake values of hydrogen at 77 K and 1 atm have been widely investigated and considered as one of the standards to compare the hydrogen-adsorption capacities of different porous MOFs [8]. These values are very useful and instructive at the early stage of exploration for hydrogen-storage materials. Several factors influencing the hydrogen uptake of porous MOFs at 77 K and 1 bar, such as surface area/pore volume, pore sizes, catenation, ligand functionalization, and unsaturated metal centers (UMCs) have been extensively studied.

Surface area/pore volume

Generally speaking, pore volume is proportional to surface area. The parameters of surface area and pore volume influencing hydrogen uptake at 77 K and 1 bar have been intensively studied in porous MOFs. However, it has been found that porous MOFs with high surface areas (above 1000 m^2/g) and large pore volumes (over 1.0 $cm^3\ g^{-1}$) show no direct correlation between surface area and hydrogen uptake [8]. For example, MOF-177 can only adsorb 0.0125 kg/kg hydrogen at 77 K, 1 atm, despite its high surface area of 5600 m^2/g and pore volume of 1.61 $cm^3\ g^{-1}$ [11]; in contrast, PCN-12, whose surface area (2425 m^2/g) and pore volume (0.94 $cm^3\ g^{-1}$) are much less than those of MOF-177, has shown the highest gravimetric uptake of hydrogen (0.0305 kg/kg), under similar conditions, among reported porous MOFs [12]. The lack of a linear correlation between hydrogen-adsorption capacity and surface area strongly indicates that low-pressure hydrogen adsorption is controlled by other factors, as discussed below.

Pore size

The low hydrogen-adsorption capacities in porous MOFs with high surface areas and large pore volumes are presumably due to the weak interactions between hydrogen molecules and the frameworks resulting from large pore sizes and spatial free void spaces. Reduction in pore size is known to enhance the interaction energy as the attractive potential fields of opposite walls overlap [8]. This has been widely explored as a strategy to enhance hydrogen–framework interactions, thereby improving hydrogen uptake [13]. Systematic investigation of pore sizes on hydrogen uptake was recently exemplified in a series of twisted borocite-type porous MOFs based on trigonal-planar carboxylate ligands and dicopper paddlewheel SBUs. Expansion of 1,3,5-benzentricarboxylate (BTC) (Scheme 1a) to triphenylene-2,6,10-tricarboxylate (TTCA) (Scheme 1b) and 4,4',4''-s-triazine-2,4,6-triyltribenzoate (TATB) (Scheme 1c) leads to proportional increase of pore sizes (8.0–11.89 and 15.16 Å) but decrease of hydrogen uptake at 77 K, 1 atm (0.0254–0.021 and 0.0162 kg/kg) [14–16]. A similar trend was also observed in a series of NbO-type porous MOFs based on tetracarboxylate organic ligands and dicopper paddlewheel SBUs, indicating an ideal pore size of ~6 Å, which may lead to optimal interaction between the dihydrogen molecule and the framework, thus maximizing the total van der Waals forces acting on dihydrogen [17].

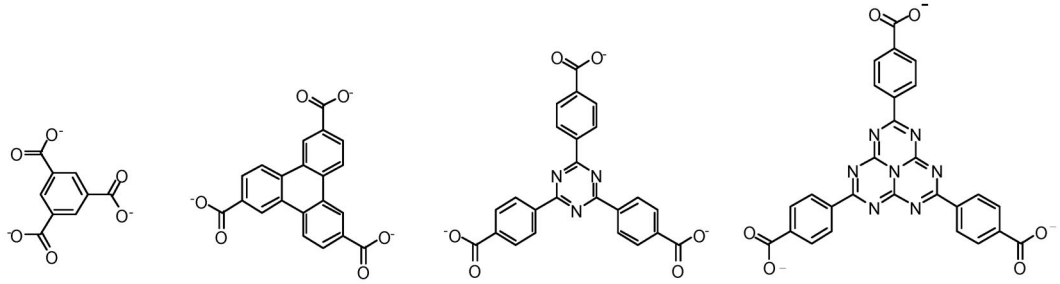

Scheme 1 Trigonal-planar carboxylate ligands: (a) BTC; (b) TTCA; (c) TATB; (d) HTB.

Catenation

Catenation, frequently encountered in porous MOFs, is the intergrowth of two or more identical frameworks [18]. It is favored by the use of longer linkers, and considered an alternative strategy for reducing pore sizes in porous MOFs [8,13]. Conceptually, a catenated porous MOF and its noncatenated counterpart can be viewed as a supramolecular pair of stereoisomers. The predictable syntheses of the catenation isomer-pairs were recently illustrated by us via using a templating strategy on the basis of copper paddlewheel SBUs and two trigonal-planar ligands (Schemes 1c,d) [16]. This allowed for the first time the evaluation of catenation as an independent criterion on the hydrogen uptake of a porous MOF. The catenation isomerism is controlled by the presence or absence of oxalic acid. Although the noncatenated form (PCN-6') has a higher overall porosity, based on the solvent-accessible volume calculated from the single-crystal X-ray structure, its catenated counterpart (PCN-6) exhibits a 41 % increase in surface area, 133 % increase in volumetric hydrogen uptake, and 29 % increase in gravimetric hydrogen uptake [16]. The hydrogen uptake enhancement resulting from catenation continues at high pressure and 77 K for catenated PCN-6 (Fig. 1a), which demonstrates a high hydrogen-adsorption capacity of 0.072 kg/kg at 50 bar compared to 0.042 kg/kg of noncatenated PCN-6 (Fig. 1b) [19]. These findings are consistent with a recent theoretical simulation, suggesting that new adsorption sites and small pores formed as a result of catenation may strengthen the overall interaction between gas molecules and the pore walls, thereby increasing the apparent surface area and hydrogen uptake [20]. The

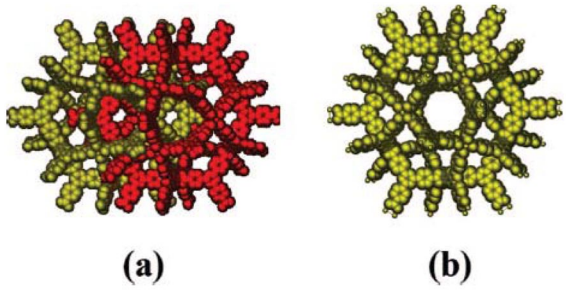

Fig. 1 (a) Catenated PCN-6. (b) Noncatenated PCN-6'. (Reprinted with permission from ref. [19]. Copyright © 2008, American Chemical Society).

mechanistic details of the interaction between hydrogen molecules and catenated PCN-6 or noncatenated PCN-6' were also elucidated through our recent inelastic neutron-scattering studies, which revealed that catenation favors hydrogen–ligand interactions at high hydrogen loadings, thus increasing hydrogen uptake in the catenated MOF compared to its noncatenated counterpart [19].

Ligand functionalization

The functionalization of organic linkers not only plays a critical role in the construction of MOFs, but also plays an important role in further enhancement of hydrogen adsorption [8,14]. Organic linkers with aromatic fragments, such as phenylene, naphthalene, and biphenylene, are widely used in the synthesis of MOFs to form a rigid three-dimensional porous framework [11,14]. Increasing the aromaticity of these organic ligands has been both theoretically predicted [21] and experimentally proved to be an effective way to enhance hydrogen-adsorption capacity [11]. A typical example is the synthesis of a series of iso-reticular MOFs (IRMOFs) which have α-Po topology based on octahedral Zn_4O SBU. It was found that the hydrogen adsorption per formula unit at 77 K and 1 bar increased with an increasing number of aromatic rings in the organic linkers. The maximum adsorption increased from 4.2 molecules of H_2 per formula unit in IRMOF-18 (2,3,5,6-tetramethylphenylene-1,4-dicarboxylate) (Scheme 2a) to 9.8 in IRMOF-13 (pyrene-2,7-dicarboxylate) (Scheme 2b). Meanwhile, the gravimetric hydrogen capacity of IRMOF-13 (0.0173 kg/kg) is almost double that of IRMOF-18 (0.0089 kg/kg) formed by 2,3,5,6-tetramethylphenylene-1,4-dicarboxylate [11,14]. These results indicate that the more aromatic rings in the organic ligands, the stronger the interactions between hydrogen and the porous MOFs. Another typical example is our recently reported NbO-type porous MOF PCN-14, which was built from an anthracene derivative, 5,5'-(9,10-anthracenediyl)di-isophthalate (Scheme 2c). PCN-14 exhibits the highest hydrogen-adsorption capacity of 0.027 kg/kg at 77 K, 1 atm among reported NbO-type porous MOFs, which were also based on tetracarboxylate organic ligands and dicopper paddlewheel SBUs [22]. The improved hydrogen uptake in PCN-14 can be ascribed to the central anthracene aromatic rings.

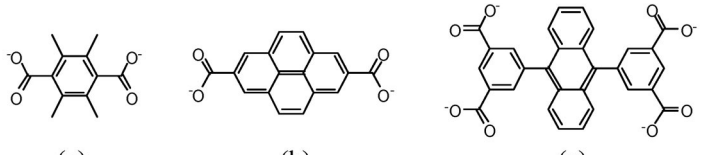

Scheme 2 (a) 2,3,5,6-tetramethylphenylene-1,4-dicarboxylate; (b) pyrene-2,7-dicarboxylate; (c) 5,5'-(9,10-anthracenediyl)di-isophthalate.

The versatility of organic ligands has provided almost infinite possibilities for the construction of porous MOFs with various topologies. Instead of simply modifying the rigid organic ligands to build MOFs with similar topology, utilizing flexible organic ligands having different stereoisomers under external stimuli can result in porous MOFs with quite different topologies. This phenomenon is referred as supramolecular isomerism. As structure determines property, supramolecular isomers are expected to exhibit different hydrogen-adsorption capacities. This has been well illustrated in a recently reported pair of porous copper MOFs based on the tetracarboxylate ligand, 5,5'-methylene-di-isophthalate (mdip), which can preserve the conformation form of C_s or C_{2v} (Fig. 2). The co-existence of C_s and C_{2v} forms for mdip allows a unique alignment of open metal sites in each cuboctahedral cage in PCN-12, which demonstrates by far the highest hydrogen uptake capacity of 0.0305 kg/kg at 77 K, 1 atm and is 27 % higher that of PCN12', in which mdip only preserves the form of C_{2v} [12]. These studies suggest that designing flexible organic linkers is a promising way to construct porous MOFs with high hydrogen uptake capacity.

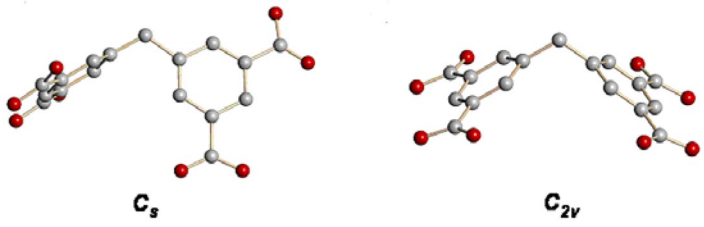

Fig. 2 Two extreme conformations of 5,5'-methylene-di-isophthalate (mdip).

Unsaturated metal centers

The impregnation of UMCs into porous MOFs is very attractive for hydrogen adsorption. One of the advantages of porous MOFs when compared to carbon materials is that metal ions incorporated in porous MOFs have higher hydrogen binding energy than carbon [13]. Recent neutron studies have revealed that hydrogen adsorption is highly dependent on the nature of the metal cation or oxide of the SBUs in porous MOFs [23]. Coordinatively, UMCs are usually very reactive and are known to play an important role in catalysis; consequently, their use in porous MOFs is a promising strategy to reach high hydrogen uptake due to their significantly high hydrogen affinity [13]. An effective way to achieve coordinative unsaturation of the metal ions is to liberate the terminal bound labile solvent (aqua) ligands by evacuation at elevated temperature (usually 100~200 °C), provided the porous framework integrity is retained after the process.

The contribution from such UMCs to hydrogen-adsorption capacity is quite remarkable [24]. This is well demonstrated by the fact that MOF-505 has a hydrogen uptake as high as 0.0247 kg/kg at 77 K and 1 atm after removal of axial aqua ligands from dicopper paddlewheel SBUs via thermal activation, generating the coordinatively unsaturated copper centers in MOF-505 [24]. Our recent studies on catenation isomers revealed that UMCs can lead to about 20 % increase in gravimetric hydrogen uptake in PCN-6 at 1 atm and 77 K [16], and comparable hydrogen uptake enhancements resulting from UMCs have also been observed in other porous MOFs [8].

Hydrogen saturation at cryo-temperatures and high-pressure hydrogen-adsorption studies at room temperature

Although extensive studies have focused on hydrogen uptake at low temperature and pressure (usually 77 K, 1 atm), escalating attention is being drawn to high-pressure hydrogen-adsorption studies because of their application potential in practical on-board hydrogen storage. In addition to evaluating high-

pressure gravimetric adsorption capacity in porous MOFs, volumetric adsorption capacity has also been widely assessed as it is another important criterion for on-board hydrogen storage.

Excess adsorption and absolute (or total) adsorption

In high-pressure studies, two concepts, namely, excess adsorption and absolute (or total) adsorption, are frequently used to describe hydrogen adsorption in porous MOFs. In brief, excess adsorption is the amount of adsorbed gas interacting with the frameworks, while absolute (or total) adsorption is the amount of gas both interacting with the frameworks and staying in pores in the absence of gas–solid interaction. The majority of the reported experimental adsorption data in the literature are excess adsorption isotherms. The absolute (or total) adsorbed amount of a porous MOF can be estimated with its crystal density derived from the single-crystal X-ray diffraction data. From the viewpoint of hydrogen storage, the total amount that a material can store or its absolute adsorption is another informative value for real application [10].

Hydrogen saturation at 77 K

Hydrogen sorption behavior at saturation is a critical parameter for judging the practicality of porous MOF materials [25]. Hydrogen saturation is very hard to achieve at room temperature due to the rapid thermal motion of dihydrogen molecules. Current research is focusing on investigating hydrogen saturation of excess uptake at 77 K. Existing studies have revealed that hydrogen saturation of excess uptake at 77 K generally scales up with surface area [8,25]. So far, the highest excess gravimetric uptake at saturation is held by MOF-177, which demonstrates an excess uptake capacity of 0.076 kg/kg at 77 K, 70 bar corresponding to a record absolute value of 0.112 kg/kg [26], and this can be ascribed to its exceptionally high surface area of 5600 m^2/g.

Most porous MOFs are very light. Generally speaking, the higher the surface area is, the lower the crystal density. In most cases, the low density decreases the volumetric hydrogen uptake of the MOF material despite its high gravimetric uptake [10]. A typical example is MOF-177, which at 77 K has the record excess gravimetric uptake of 0.076 kg/kg at saturation and the highest total capacity of 0.112 kg/kg at 78 bar benefiting from its high Langmuir surface area of 5640 m^2/g [26]. Its low crystallographic density of 0.427 g cm^{-3}, however, leads to the volumetric storage densities of just 0.032 kg/l (excess) and 0.048 kg/l (total) [26], which are significantly lower than those of PCN-6 (0.042 kg/l for excess uptake and 0.053 kg/l for total uptake at 77 K, 50 bar) in spite of its much lower surface area (3800 m^2/g) compared to MOF-177 [19]. A compromise between the surface area and crystal density thus should be met in search of porous MOF material with both high gravimetric and volumetric hydrogen uptake.

Existing reported hydrogen-adsorption data of porous MOFs at 77 K and high pressure indicate that porous MOFs could achieve or even surpass DOE 2010 target values for both gravimetric and volumetric hydrogen storage, promising their potential as cryogenic hydrogen-storage media. However, the cost of the cryo-storage vessel precludes its practical on-board application, and porous MOFs with high hydrogen uptake near-ambient temperature are urgently needed.

High-pressure hydrogen adsorption at room temperature

Room-temperature hydrogen-adsorption studies under high pressure have been carried out for porous MOF materials. Unfortunately, these materials have very low hydrogen uptake at room temperature (less than 0.015 kg/kg) [8]. High surface area alone is insufficient to achieve high capacity for ambient-temperature storage, albeit it can lead to high hydrogen saturation uptake at 77 K. Small pore size seems necessary for ambient-temperature hydrogen adsorption due to the enhanced interaction energy [8]. This is well illustrated in [Cu(hfipbb)(H_2hfipbb)$_{0.5}$], a microporous MOF which contains pores of two types: small (~3.5 ↔ 3.5 Å) and large (5.1 ↔ 5.1 Å). At room temperature and 48 atm, it can adsorb ~0.01 kg/kg of hydrogen [27], which is more than three times that of MOF-5 (0.0028 kg/kg, 60 atm) which contains pore size of ~7.7 ↔ 7.7 Å and has a high surface area of 2300 m^2/g [8].

An effective way to reduce pore size is utilizing interpenetration (or catenation), which has been proposed as a strategy to improve hydrogen uptake. A typical example of this method is $Zn_4O(L^1)_3$ (L^1 = 6,6'-dichloro-2,2'-diethoxy-1,1'-binaphthyl-4,4'-dibenzoate) (Scheme 3a), which is fourfold interpenetrated with open channels of less than 5 Å, and a Brunauer–Emmett–Teller (BET) surface area of only 502 $m^2\ g^{-1}$; this material adsorbs 0.0112 kg/kg of hydrogen at room temperature and 48 bar, among the highest of reported porous MOF materials [28].

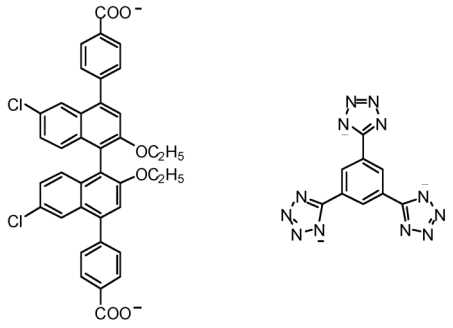

Scheme 3 (a) 6,6'-dichloro-2,2'-diethoxy-1,1'-binaphthyl-4,4'-dibenzoate; (b) 1,3,5-benzenetristetrazolate (btt).

The introduction of UMCs into MOFs has been known as one of the most promising ways to improve hydrogen affinity. The ability of UMC-containing porous MOFs to adsorb significant amount of hydrogen is well demonstrated by Long and co-workers in the porous MOF $Mn_3[(Mn_4Cl)_3(btt)_3(CH_3OH)_{10}]_2$ (btt = 1,3,5-benzenetristetrazolate) (Scheme 3b). Upon thermal activation, this porous MOF can adsorb 0.0014 kg/kg of hydrogen at 298 K and 90 bar. This high uptake capacity can be partially ascribed to the exposed Mn^{2+} sites within the framework which interact strongly with H_2 molecules [29].

Despite the rapidly growing efforts on the investigation of hydrogen adsorption in porous MOFs, the near-ambient-temperature hydrogen uptake of these materials falls far short of the 2010 DOE targets. On-board hydrogen storage using adsorptive materials for fuel-cell-powered vehicles remains very much a challenge.

Hydrogen-adsorption enthalpy

The major hurdle limiting hydrogen uptake at ambient temperature is the weak interaction between hydrogen molecules and the frameworks of porous MOFs. Hydrogen binding energy or hydrogen affinity can be quantitatively estimated by measuring the isosteric heats of adsorption of hydrogen or the hydrogen-adsorption enthalpy, H_{ads}. Recently, a desired binding energy of ca. 20 kJ/mol in the overall hydrogen loading range has been proposed for room-temperature hydrogen storage [30]. Various strategies to be described below have been explored to increase the hydrogen-adsorption enthalpy to approach this value.

Utilizing small pore sizes comparable to the kinetic diameter of a dihydrogen molecule is efficient to enhance hydrogen-adsorption enthalpy. An example of this was found in a microporous magnesium MOF; this material contains very small pores of ~3.5 Å, and exhibits a high hydrogen-adsorption enthalpy of 9.5 kJ/mol at low hydrogen coverage [31].

The creation of UMCs in porous MOFs is considered one of the most effective strategies to increase hydrogen-adsorption enthalpy. The exposure of UMCs by removing the coordinated labile solvent ligands using thermal activation in the porous MOFs $Mn_3[(Mn_4Cl)_3(btt)_3(CH_3OH)_{10}]_2$ and

$NaNi(sip)_2$, led to high-adsorption enthalpies of 10.1 kJ/mol at low hydrogen coverage [29,32]. A high-adsorption enthalpy of over 12 kJ/mol was achieved in a mixed copper–zinc porous MOF in which Pyen ligands with open copper centers serve as pillars [33]. The effects of different UMCs on hydrogen-adsorption enthalpies have recently been investigated in a series of isomorphous structures revealed that open nickel centers possess the highest hydrogen binding energy (13.5 kJ/mol) compared to other first transition metals and magnesium [34].

Instead of utilizing thermal activation to achieve coordinative unsaturation by removal of one or more ligands from a metal center, coordinatively UMCs can be accomplished via a biomimetic approach by creating entatic metal centers (EMCs) as recently illustrated by us in the porous MOF PCN-9 [35]. In bioinorganic chemistry, protein EMCs are enforced by surrounding polypeptides; they are imposed into an unusual coordination geometry to enhance their reactivity in electron transfer, substrate binding, or catalysis. Similarly, due to the specific geometric requirements of the ligands and SBUs in a porous MOF, EMCs can be created and are expected to have high hydrogen affinity. By mimicking the coordinatively unsaturated iron active center of hemoglobin, the hemoglobin-like entatic cobalt centers in PCN-9 exhibit high hydrogen affinity with adsorption enthalpy of 10.1 kJ/mol at low coverage (Fig. 3). The accessibility of those entatic cobalt centers was also probed by carbon monoxide molecules via IR spectroscopy studies. The investigation of a series of PCN-9s with different EMCs revealed that entatic cobalt center has the highest hydrogen affinity compared to entatic iron and manganese centers [36].

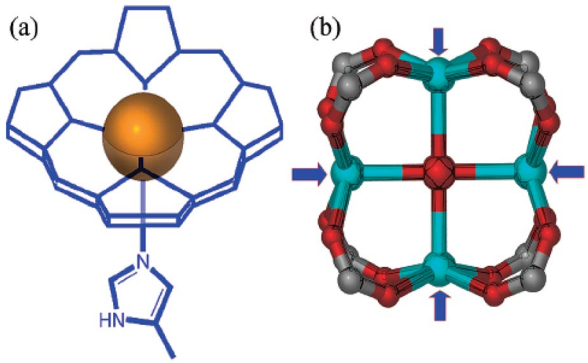

Fig. 3 (a) The active center of hemoglobin (the orange sphere represents an Fe atom). (b) The $M_4(\mu_4\text{-O})(\text{carboxylate})_4$ SBU, with arrows indicating the displaced EMCs. (M = Co, Fe, Mn). Color scheme: C, gray; M, aqua; and O, red. (Reprinted with permission from ref. [36], copyright © 2009, American Chemical Society).

Cation exchange in an anionic framework is yet another way to achieve coordinative unsaturation. The study of cation-exchange on hydrogen-adsorption enthalpy and capacity was recently performed in an anionic porous MOF $Mn_3[(Mn_4Cl)_3(btt)_3(CH_3OH)_{10}]_2$. The findings revealed that the Mn^{2+}-, Fe^{2+}-, and Co^{2+}-exchanged frameworks demonstrated the strongest H_2 binding among all the cations assessed. The Co^{2+}-exchanged framework exhibited a remarkable hydrogen-adsorption enthalpy of 10.5 kJ/mol at zero coverage [37].

Although porous MOFs with UMCs have exhibited significantly higher hydrogen-adsorption enthalpies compared to other porous materials such as inorganic zeolites, activated carbon, carbon nanotubes, and porous organic polymers, those values are still far away from the desired binding energy of ca. 20 kJ/mol in the overall hydrogen loading range. Exploration of porous MOFs with high hydrogen uptake at near-ambient temperatures for on-board storage applications still has a long way to go.

Hydrogen spillover

One intriguing method for hydrogen-adsorption enhancement at near-ambient temperatures is the secondary hydrogen spillover. It consists of the dissociative chemisorption of hydrogen on a metal catalyst with the subsequent migration of atomic hydrogen to the surface of a carrier contacting the metal (primary hydrogen receptor) and then to the second carrier (secondary receptor) [38]. Li and Yang demonstrated that mechanically mixing 5 % platinum on activated carbon with porous MOFs, followed by melting and subsequent carbonization of an amount of sucrose with the MOF, could give rise to materials with a hydrogen uptake capacity up to 0.03~0.04 kg/kg at 298 K and 10 MPa. In the meantime, the hydrogen-adsorption enthalpies were enhanced to 20~23 kJ/mol, which achieves the desired enthalpy of 20 kJ/mol. These results are very encouraging, and the secondary hydrogen spillover technique indeed shows great potential for achieving the 2010 DOE gravimetric target of 0.045 kg/kg for hydrogen storage. However, difficulties in reproducing some of the experimental results cast a shadow on the outlook of such a fascinating technique [8].

METHANE-STORAGE APPLICATION OF POROUS MOFs

As with hydrogen, methane is considered an ideal energy gas for future applications. Compared to petroleum oil, methane can provide much more energy because of its higher hydrogen-to-carbon ratio and has much lower carbon emission, and it appears to be a more promising alternative for mobile applications in terms of near-term practical utilization and innovations necessary for commercialization [39].

Methane-storage goals

Methane is the primary component of natural gas; as such, an extensive system of collection, purification, and distribution infrastructure already exists, capable of delivering methane to the majority of homes and businesses in the United States and many other countries worldwide. Deposits of methane-containing natural gas are more widespread globally than those of petroleum, and its refinement (purification) to an energy fuel is much simpler than that of crude petroleum oil to gasoline or diesel fuels. Methane is also produced by decomposition of organic waste and by bacteria in the guts of ruminants and termites. In fact, methane and natural gas are often considered waste products in crude oil collection and refining and other industrial processes, and are often burned off in giant flares with no secondary energy capture. Although compressed natural gas (CNG) vehicles already exist, current vehicles store the methane CNG in high-pressure (greater than 200 atm) tanks which are heavy and potentially explosive [39]. To address the needs for better methane-storage technology, the DOE has set targets for methane-storage systems at 180 v(STP)/v (STP equivalent of methane per volume of adsorbent material storage system) under 35 bar and near-ambient temperature, with the energy density of adsorbed natural gas comparable to that of current CNG technology [40].

Methane storage in porous MOFs

Porous MOFs are a relative newcomer to the field of methane adsorbents. While carbon materials have been extensively studied for methane storage since the early 1990s, the first reported measurement of methane uptake by a porous MOF dates back to as early as a 1997 report by Kitagawa and co-workers albeit with very low methane uptake [41]. However, the field of methane storage on MOFs has not expanded as quickly as the hydrogen-storage field, and studies on methane storage in porous MOFs are by far less numerous than hydrogen, and to date there have been just about 30 reports of methane adsorption in porous MOFs [39].

As opposed to hydrogen storage, methane-storage targets set by DOE are only for volumetric capacity in the unit of v(STP)/v [40]. However, gravimetric capacities in units of cm^3/g or mmol/g have

been regularly reported, and these values are very useful for the exploration of methane-storage materials. To date, the reported volumetric storage capacities of porous MOFs are estimated from gravimetric values using their crystallographic densities.

As in the case of hydrogen storage, a variety of factors influence the methane uptake capacities of porous MOFs, namely, surface areas, pore sizes, ligand functionalization, and heats of adsorption (with contributions from both framework topology and chemical functionality), etc. [39]. For example, the impact of interpenetration was investigated by Kitagawa and co-workers on a series of azopyridine-based MOFs, with the highest of the series adsorbing ~60 v(STP)/v [42].

The ability of IRMOF-6 to adsorb a higher amount of methane than the other members of the IRMOF series was attributed to both the accessible surface area and the functionality of the ligand: in IRMOF-6, the phenyl ring of the typical bdc ligand was modified to generate 1,2-cyclobutane-3,6-benzenedicarboxylate (Scheme 4a). The resulting porous MOF was found to uptake 155 v(STP)/v (or 240 cm^3/g) methane at 298 K and 36 atm [43], considerably higher than any zeolite material or any other porous MOF at the time, particularly in terms of gravimetric capacity. Theoretical simulations [44] suggested that further functionalization of the ligand by insertion of an anthracene ring (Scheme 4b) would enhance methane uptake further, perhaps within reach of the DOE target. Attempt to synthesize this proposed porous MOF, however, resulted in a material with a very small amount of methane uptake, owing to the ultramicroporous nature of the porous MOF, with pores too small to accommodate methane [45].

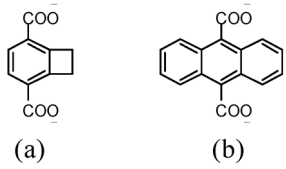

Scheme 4 (a) 1,2-cyclobutane-3,6-benzenedicarboxylate; (b) 9,10-anthracenedicarboxylate.

Nevertheless, the problems associated with extremely small pores have recently been triumphed by extending the ligand with additional phenyl rings to form 5,5'-(9,10-anthracenediyl)-diisophthalate (adip) (Scheme 2c) in our recent work. The resulting porous MOF, dubbed PCN-14, was found to contain nanoscopic cages of a size (Fig. 4) suitable for methane storage, with an absolute adsorption capacity of 230 v(STP)/v (excess: 220 v(STP)/v) 28 % higher than the DOE target, at 290 K and 35 bar. In addition, the heats of adsorption of methane on the framework are ~30 kJ/mol at low methane coverage, higher than any other reported porous MOF—this indicates the validity of using H_{ads} as a bench-

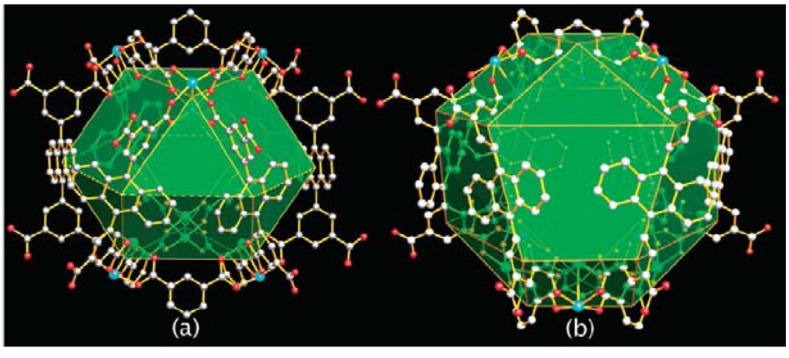

Fig. 4 Nanoscopic cages in PCN-14, which exhibits by far the highest methane uptake capacity. (Reprinted with permission from ref. [46], copyright © 2008, American Chemical Society).

mark for evaluating potential saturation uptake at room temperature. PCN-14 holds the current record for methane storage, and represents the first case surpassing the DOE target for porous MOFs [46].

To elucidate the location of methane adsorption sites together with methane–framework interactions in porous MOFs, neutron powder diffraction has recently been employed for the studies of CD_4 adsorption in MOF-5 [47] and a series of isomorphous porous MOFs with different UMCs [48]. Information derived from these studies is very useful for future design of new porous MOFs with high methane-storage capacities. However, to further illustrate structure–performance correlations, systematic investigation of the impact from other factors such as pore size, ligand functionalization, etc. on methane uptakes in porous MOFs are needed, and this necessitates more studies to screen existing porous MOFs as well as to develop more new structures.

SELECTIVE GAS ADSORPTION APPLICATION OF POROUS MOFS

Gas separation and purification are important and energy-consuming in industrial applications. A few of the commercially most important gas separation challenges are: N_2/O_2 separation, N_2/CH_4 separation for natural gas upgrading, and CO removal from H_2 for fuel cell applications [5,49]. Although inorganic zeolites and porous carbon materials can be applied with some success, new adsorbents are still needed to optimize these separation processes to make them commercially more attractive. As a new type of zeolite analogues, porous MOFs feature amenability to design, tunable pore size, and functionalizable pore walls; these characteristics offer them great potential in selective adsorption of gases [50].

Molecular-sieving effect in porous MOFs

The molecular-sieving effect arises when molecules of appropriate size and shape are allowed to enter the open channels of an adsorbent, while other molecules are excluded. It accounts for the underlying principle for most selective gas-adsorption processes in porous materials with uniform micropores [49].

It is essential to limit the pore size of an adsorbent for effective gas separation. To this point, apertures of porous MOFs can be rationally tuned to a certain size for selective adsorption of specific gas molecules.

Utilizing short bridging ligands is a good way to restrict pore sizes of porous MOFs for gas separation. This was exemplified in a microporous manganese formate MOF. The short length of the formate leads to very small aperture size, which can discriminate H_2 from N_2, and CO_2 from CH_4 [51]. In addition, success of confining the pore size to around 3.5 Å by using 2,6-naphthalenedicarboxylic acid was achieved in a microporous magnesium MOF. The magnesium MOF exhibited the capability of selective uptake of H_2 or O_2 over N_2 or CO [31]. Similar molecular-sieving effect was also observed in a 2,4-pyridinedicarboxylate-based cobalt MOF (CUK-1), which could separate H_2 from N_2, O_2 from N_2 and Ar, and CO_2 from CH_4 [52].

As an alternative strategy, increasing the bulkiness of the struts to constrict the apertures of porous MOFs was well illustrated by us in the construction of a zinc microporous MOF, PCN-13. PCN-13 was built from a bulky ligand 9,10-anthracenedicarboxylate (adc). Due to the bulkiness of adc, the pore size of PCN-13 is constricted to ~3.5 Å ↔ 3.5 Å, which allows H_2 and O_2 to pass through the pores but excludes N_2 and CO [45].

Interpenetration is well known as an effective way to reduce pore size of porous MOFs, and has been recently employed to confine the pore size for selective adsorption of gas molecules. It has been well illustrated that doubly interpenetrated primitive cubic nets based on bidentate pillar linkers and bicarboxylates could be rationally designed for selective gas adsorption. The microporous MOF $Cu(FMA)(4,4'\text{-Bpe})_{0.5}$ [FMA = fumarate (Scheme 5a); 4,4'-Bpe = trans-bis(4-pyridyl)ethylene (Scheme 5b)] was constructed by the incorporation of the bicarboxylate FMA and bidentate pillar linker 4,4'-Bpe, and its pore size was tuned by double framework interpenetration to ~3.6 Å, which exhibits

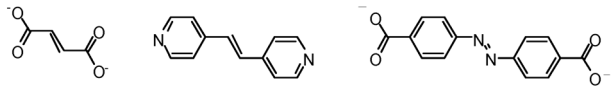

(a) (b) (c)

Scheme 5 (a) fumarate; (b) *trans*-bis(4-pyridyl)ethylene; (c) 4,4'-azobenzenedicarboxylate.

selective adsorption of H_2 over Ar, N_2, and CO [53]. By increasing the length of the bicarboxylates and bidentate pillar linkers, Chen et al. introduced triple interpenetration in the microporous MOF Zn(ADC)(4,4'-Bpe)$_{0.5}$ [ADC = 4,4'-azobenzenedicarboxylate (Scheme 5a)], which can distinguish H_2 from N_2 and CO [54].

Linking interpenetration with coordinative bonds cannot only further confine the pore size, but also improve the thermal stability of a porous MOF. This has been well demonstrated in our recently reported porous MOF, PCN-17 which possesses doubly interpenetrated frameworks coordinatively linked by the in situ generated sulfate ligands. The coordinatively linked interpenetration offers PCN-17 high thermal stability of up to 480 °C while maintaining permanent porosity as well as capability to selectively adsorb dihydrogen and dioxygen over dinitrogen and carbon monoxide [55].

Porous MOFs for kinetic separation application

Different from the molecular-sieving effect, kinetic separation is achieved by virtue of the differences in diffusion rates of different molecules. Kinetic separation is of great importance in industry applications, particularly chromatography applications [49].

The separation of mixed C_8 alkylaromatic compounds (*p*-xylene, *o*-xylene, *m*-xylene, and ethylbenzene) is one of the most challenging separations in chemical industry due to the similarity of their boiling points [56]. This separation is currently performed by cation-exchanged zeolites X and Y in industry [56]; however, adsorbents with improved separation efficiency are still needed. Recently, Vos et al. for the first time investigated the adsorption and separation of a mixture of C_8 alkylaromatic compounds using three porous MOFs: HKUST-1, MIL-53, and MIL-47 in the liquid phase. Through chromatographic experiments, it was concluded that MIL-47 has the highest potential for the separation of C_8 alkylaromatic compounds among the three investigated MOFs. Compared with currently used zeolites, MIL-47 displays high uptake capacity and high selectivity, which are advantageous for its future practical application in industry [57].

The separation of hexane isomers to boost octane ratings in gasoline represents a very important process in the petroleum industry [58]. This is achieved using the high energy-consuming method of cryogenic distillation, albeit some alternative novel materials and technologies are now under rapid development. By making use of the pore space to capture and discriminate hexane isomers, porous MOFs have the potential to separate hexane isomers. This was well illustrated in the kinetic separation of hexane isomers by using the three-dimensional microporous MOF, Zn(BDC)(dabco)$_{0.5}$. The MOF Zn(BDC)(dabco)$_{0.5}$ contains three-dimensional intersecting pores of about 7.5 ↔ 7.5 Å along axis [100] and pores of 3.8 ↔ 4.7 Å along axes [010] and [001]. By making use of the narrow channels of 3.8 ↔ 4.7 Å to exclusively take up linear nHEX while blocking branched hexane isomers, this MOF was successfully used in the kinetic separation of hexane isomers by fixed-bed adsorption. It exhibited extraordinary separation selectivity to separate branched hexane isomers from linear nHEX. This represented the first example of using microporous MOFs for the kinetic separation of hexane isomers, demonstrating great potential for applications in the very important industrial process of hexane-isomers separation [59].

Another important process to boost octane ratings in gasoline is the separation of alkane isomers, which is currently practiced by using some narrow pore zeolites [60]. Chen et al. recently demonstrated the application of a microporous MOF (MOF-508) packed column in the gas chromatography (GC)

separation of alkanes. MOF-508 contains one-dimensional pores of 4.0 ↔ 4.0 Å, which can selectively accommodate linear alkanes and discriminate branched alkanes. The subtle matching of the size and shape of the alkanes with the micropores of MOF-508 leads to different van der Waals interactions, thus resulting in selective GC separation of alkanes in the MOF-508 column [61].

One of the most difficult chemical separations is propane/propylene, because of their very close relative volatilities and molecular sizes. A promising solution for this issue has recently been demonstrated in a series of zinc imidazolate zeolitic framework, which are capable of kinetic separation of propane and propylene [62].

Mesh-adjustable molecular sieves (MAMSs)

Inorganic zeolite molecular sieves are currently the most used adsorbents in industry for gas separations [49]. The rigidity of the bonds in zeolites affords them with fixed mesh sizes. This is advantageous when the mesh size precisely fits the separation needs. However, when the size disparity of the two gases is very small, a zeolite molecular sieve with the precise mesh size is not always readily available. In such cases, MAMSs that can always meet the separation needs are highly desirable.

The first mesh-adjustable molecular sieve, MAMS-1, was recently successfully constructed by us based on the amphiphilic ligand 5-*tert*-butyl-1, 3-benzenedicarboxylate (BBDC) (Scheme 6a) [63]. MAMS-1 is a trilayer structure, and consists of hydrophilic channels and hydrophobic chambers. The hydrophilic channel and hydrophobic chamber are interconnected with each other through a pair of BBDC ligands at their interface. Variable-temperature gas adsorption studies on MAMS-1 revealed that it exhibited temperature-induced molecular-sieving effect, and its mesh range falls between 2.9 and 5.0 Å. When the temperature is precisely controlled, any mesh size within this range can be accurately attained. Mechanistic studies suggested that the hydrophobic chambers are the major storage room for gas molecules, which have to go through the fully activated hydrophilic channels to enter the hydrophobic chambers. The BBDC ligands at the interface of hydrophilic channels and hydrophobic chambers play the role of the gates, which open linearly with increasing temperatures to gradually let gas molecules of certain sizes enter the hydrophobic chambers (Fig. 5). The extension of BBDC ligand to the BBPDC ligand (Scheme 6b), when reacted with different metal ions under solvothermal conditions generates a series of new MAMSs with similar molecular-sieving effects to those observed in MAMS-1 [64]. For all of the MAMSs, there exists a linear relationship between mesh size and temperature, $D = D_0 + \alpha T$ (D = mesh size at temperature T K, D_0 = mesh size at 0 K, and α-constant), D_0 and α are only related to the tert-butyl group. Adjusting D_0 and α is expected to result in some new MAMSs which might be omnipotent for gas separation at near-ambient temperatures.

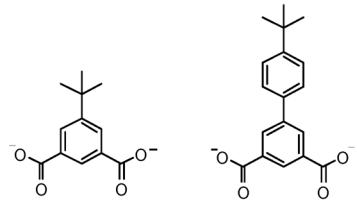

(a) (b)

Scheme 6 (a) BBDC ligand; (b) BBPDC ligand.

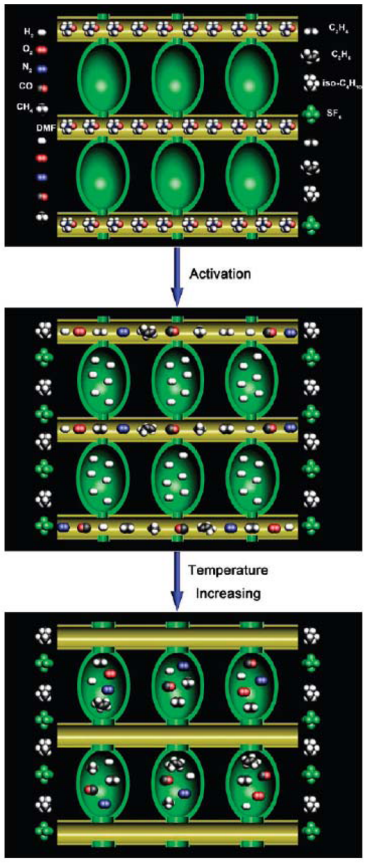

Fig. 5 Schematic representation of the mechanism of the temperature-dependent gating effects in MAMSs. (Reprinted with permission from ref. [63], Copyright © 2009, American Chemical Society).

CONCLUSIONS

As a relatively new class of materials, porous MOFs will continue to attract interest and inquiry by both academia and industry. They exhibit great potential for hydrogen and methane storage in energy applications as well as gas separation and purification in industrial applications. The unique ability to adjust the pore size and alter the pore wall functionality allows researchers to focus on those factors which hold to the most promise, increasing both the volume available for storage and the affinity of the framework for the stored gas. In particular, as clean and alternative fuels such as hydrogen and methane continue to be developed in automotive and other applications, the needs for effective storage technologies will continue to increase, and porous MOFs are well positioned to remain at the forefront of this research.

ACKNOWLEDGMENTS

I would first like to thank IUPAC for giving me the precious opportunity to present this work. I would also like to thank the Dissertation Scholarship from Miami University and the Director's Postdoctoral Fellowship from Argonne National Laboratory. Last but not least, I would like to express my deepest appreciation to my Ph.D. advisor, Prof. Hong-Cai Zhou, for his excellent education, tremendous support, and constant encouragement throughout my graduate career and beyond. Financial support for my

Ph.D. research work is from Miami University, NSF, and DOE, all of which I would like to acknowledge here as well.

REFERENCES

1. J. R. Long, O. M. Yaghi. *Chem. Soc. Rev.* **38**, 1213 (2009).
2. D. J. Tranchemontagne, J. L. Mendoza-Cortes, M. O'Keeffe, O. M. Yaghi. *Chem. Soc. Rev.* **38**, 1257 (2009).
3. G. Férey. *Chem. Soc. Rev.* **37**, 191 (2008).
4. S. Ma. Ph.D. Dissertation, Miami University (2008).
5. S. Ma, C. D. Collier, H.-C. Zhou. "Design and construction of metal-organic frameworks for hydrogen storage and selective gas adsorption", in *Design and Construction of Coordination Polymers*, M. Hong (Ed.), John Wiley, New York (2009).
6. DOE Office of Energy Efficiency and Renewable Energy Hydrogen. Fuel Cells & Infrastructure Technologies Program Multi-Year Research, Development and Demonstration Plan, available at: <http://www.eere.energy.gov/hydrogenandfuelcells/mypp>.
7. U.S. Department of Energy. Targets for on-board hydrogen storage systems: Current R&D focus is on 2015 targets with potential to meet ultimate targets (<http://www1.eere.energy.gov/hydrogenandfuelcells/storage/current_technology.html>).
8. D. J. Collins, H.-C. Zhou. *J. Mater. Chem.* **17**, 3154 (2007).
9. N. L. Rosi, J. Eckert, M. Eddaoudi, D. T. Vodak, J. Kim, M. O'Keefe, O. M. Yaghi. *Science* **300**, 1127 (2003).
10. L. J. Murray, M. Dinca, J. R. Long. *Chem. Soc. Rev.* **38**, 1294 (2009).
11. J. L. C. Rowsell, A. R. Millward, K. S. Park, O. M. Yaghi. *J. Am. Chem. Soc.* **126**, 5666 (2004).
12. X.-S. Wang, S. Ma, P. M. Forster, D. Yuan, J. Eckert, J. J. Lopez, B. J. Murphy, J. B. Parise, H.-C. Zhou. *Angew. Chem., Int. Ed.* **47**, 7263 (2008).
13. J. L. C. Rowsell, O. M. Yaghi. *Angew. Chem., Int. Ed.* **44**, 4670 (2005).
14. J. L. C. Rowsell, O. M. Yaghi. *J. Am. Chem. Soc.* **128**, 1304 (2006).
15. X.-S. Wang, S. Ma, D. Yuan, J. W. Yoon, Y. K. Hwang, J.-S. Chang, X. Wang, M. R. Jørgensen, Y.-S. Chen, H.-C. Zhou. *Inorg. Chem.* **48**, 7519 (2009).
16. S. Ma, D. Sun, M. Ambrogio, J. A. Fillinger, S. Parkin, H.-C. Zhou. *J. Am. Chem. Soc.* **129**, 1858 (2007).
17. X. Lin, J. Jia, X. Zhao, K. M. Thomas, A. J. Blake, G. S. Walker, N. R. Champness, P. Hubberstey, M. Schröder. *Angew. Chem., Int. Ed.* **45**, 7358 (2006).
18. S. R. Batten, R. Robson. *Angew. Chem., Int. Ed.* **37**, 1460 (1998).
19. S. Ma, J. Eckert, P. M. Forster, J. W. Yoon, Y. K. Hwang, J.-S. Chang, C. D. Collier, J. B. Parise, H.-C. Zhou. *J. Am. Chem. Soc.* **130**, 15896 (2008).
20. D. H. Jung, D. Kim, T. B. Lee, S. B. Choi, J. H. Yoon, J. Kim, K. Choi, S.-H. Choi. *J. Phys. Chem. B* **110**, 22987 (2006).
21. S. S. Han, W. A. Goddard III. *J. Am. Chem. Soc.* **129**, 8422 (2007).
22. S. Ma, J. M. Simmons, D. Sun, D. Yuan, H.-C. Zhou. *Inorg. Chem.* **48**, 5263 (2009).
23. J. L. C. Rowsell, J. Eckert, O. M. Yaghi. *J. Am. Chem. Soc.* **127**, 14904 (2005).
24. B. Chen, N. W. Ockwig, A. R. Millward, D. S. Contreras, O. M. Yaghi. *Angew. Chem., Int. Ed.* **44**, 4745 (2005).
25. A. G. Wong-Foy, A. J. Matzger, O. M. Yaghi. *J. Am. Chem. Soc.* **128**, 3494 (2006).
26. H. Furukawa, M. A. Miller, O. M. Yaghi. *J. Mater. Chem.* **17**, 3197 (2007).
27. L. Pan, M. B. Sander, X. Huang, J. Li, M. R. Smith, E. W. Bittner, B. C. Bockrath, J. K. Johnson. *J. Am. Chem. Soc.* **126**, 1308 (2004).

28. B. Kesanli, Y. Cui, M. R. Smith, E. W. Bittner, B. C. Bockrath, W. Lin. *Angew. Chem., Int. Ed.* **44**, 72 (2005).
29. M. Dincă, A. Dailly, Y. Liu, C. M. Brown, D. A. Neumann, J. R. Long. *J. Am. Chem. Soc.* **128**, 16876 (2006).
30. S. K. Bhatia, A. L. Myers. *Langmuir* **22**, 1688 (2006).
31. M. Dincă, J. R. Long. *J. Am. Chem. Soc.* **127**, 9376 (2005).
32. P. M. Forster, J. Eckert, B. D. Heiken, J. B. Parise, J. W. Yoon, S. H. Jhung, J. S. Chang, A. K. Cheetham. *J. Am. Chem. Soc.* **128**, 16846 (2006).
33. B. Chen, X. Zhao, A. Putkham, K. Hong, E. B. Lobkovsky, E. J. Hurtado, A. J. Fletcher, K. M. Thomas. *J. Am. Chem. Soc.* **130**, 6411 (2008).
34. W. Zhou, H. Wu, T. Yildirim. *J. Am. Chem. Soc.* **130**, 15268 (2008).
35. S. Ma, H.-C. Zhou. *J. Am. Chem. Soc.* **128**, 11734 (2006).
36. S. Ma, D. Yuan, J. S. Chang, H.-C. Zhou. *Inorg. Chem.* **48**, 5398 (2009).
37. M. Dincă, J. R. Long. *J. Am. Chem. Soc.* **129**, 11172 (2007).
38. Y. Li, R. T. Yang. *J. Am. Chem. Soc.* **128**, 8136 (2006).
39. D. J. Collins, S. Ma, H.-C. Zhou. "Hydrogen and methane storage in MOFs", in *Metal-Organic Frameworks: Design and Application*, L. MacGillivray (Ed.), Wiley-VCH, Weinheim (2009).
40. T. Burchell, M. Rogers. *SAE Tech. Pap. Ser.* 2000 (2000).
41. M. Kondo, T. Yoshitomi, K. Seki, H. Matsuzaka, S. Kitagawa. *Angew. Chem., Int. Ed.* **36**, 1725 (1997).
42. M. Kondo, M. Shimamura, S.-i. Noro, S. Minakoshi, A. Asami, K. Seki, S. Kitagawa. *Chem. Mater.* **12**, 1288 (2000).
43. M. Eddaoudi, J. Kim, N. Rosi, D. Vodak, J. Wachter, M. O'Keeffe, O. M. Yaghi. *Science* **295**, 469 (2002).
44. T. Düren, L. Sarkisov, O. M. Yaghi, R. Q. Snurr. *Langmuir* **20**, 2683 (2004).
45. S. Ma, X. S. Wang, C. D. Collier, E. S. Manis, H. C. Zhou. *Inorg. Chem.* **46**, 8499 (2007).
46. S. Ma, J. Eckert, P. M. Forster, J. W. Yoon, Y. K. Hwang, J.-S. Chang, C. D. Collier, J. B. Parise, H.-C. Zhou. *J. Am. Chem. Soc.* **130**, 15896 (2008).
47. H. Wu, W. Zhou, T. Yildirim. *J. Phys. Chem. C* **113**, 3029 (2009).
48. H. Wu, W. Zhou, T. Yildirim. *J. Am. Chem. Soc.* **131**, 4995 (2009).
49. R. T. Yang. *Gas Adsorption by Adsorption Processes*, Butterworth, Boston (1997).
50. J.-R. Li, R. J. Kuppler, H.-C. Zhou. *Chem. Soc. Rev.* **38**, 1477 (2009).
51. D. N. Dybtsev, H. Chun, S. H. Yoon, D. Kim, K. Kim. *J. Am. Chem. Soc.* **126**, 32 (2004).
52. S. M. Humphrey, J.-S. Chang, S. H. Jhung, J. W. Yoon, P. T. Wood. *Angew. Chem., Int. Ed.* **46**, 272 (2007).
53. B. Chen, S. Ma, F. Zapata, F. R. Fronczek, E. B. Lobkovsky, H.-C. Zhou. *Inorg. Chem.* **46**, 1233 (2007).
54. B. Chen, S. Ma, E. J. Hurtado, E. B. Lobkovsky, H.-C. Zhou. *Inorg. Chem.* **46**, 8490 (2007).
55. S. Ma, X.-S. Wang, D. Yuan, H.-C. Zhou. *Angew. Chem., Int. Ed.* **47**, 4130 (2008).
56. R. Hulme, R. Rosensweig, D. Ruthven. *Ind. Eng. Chem. Res.* **30**, 752 (1991).
57. L. Alaerts, C. E. A. Kirschhock, M. Maes, M. A. van der Veen, V. Finsy, A. Depla, J. A. Martens, G. V. Baron, P. A. Jacobs, J. F. M. Denayer, D. E. De Vos. *Angew. Chem., Int. Ed.* **46**, 4293 (2007).
58. S. W. Sohn. "Kerosene ISOSIV process for production of normal paraffins", in *Handbook of Petroleum Refining Processes*, 3rd ed., R. A. Meyers (Ed.), McGraw-Hill, New York (2004).
59. P. S. Barcia, F. Zapata, J. A. C. Silva, A. E. Rodrigues, B. Chen. *J. Phys. Chem. B* **111**, 6101 (2007).
60. S. Kulprathipanja, R. W. Neuzil. U.S. Patent 4 444 445 (1984).
61. B. Chen, C. Liang, J. Yang, D. S. Contreras, Y. L. Clancy, E. B. Lobkovsky, O. M. Yaghi, S. Dai. *Angew. Chem., Int. Ed.* **45**, 1390 (2006).

62. K. Li, D. H. Olson, J. Seidel, T. J. Emge, H. Gong, H. Zeng, J. Li. *J. Am. Chem. Soc.* **131**, 10368 (2009).
63. S. Ma, D. Sun, X.-S. Wang, H.-C. Zhou. *Angew. Chem., Int. Ed.* **46**, 2458 (2007).
64. S. Ma, D. Sun, D. Yuan, X.-S. Wang, H.-C. Zhou. *J. Am. Chem. Soc.* **131**, 6445 (2009).